Laser-noise-induced population fluctuations in two- and three-level systems

Th. Haslwanter, H. Ritsch, J. Cooper, and P. Zoller*
Joint Institute for Laboratory Astrophysics, University of Colorado and National Bureau of Standards, Campus Box 440, Boulder, Colorado 80309-0440
(Received 1 June 1988)

Significant fluctuations, above the shot-noise limit, have been observed in the intensity of fluorescent light scattered from atoms excited by an intense noisy laser, where a central role is played by the nonlinearity of the atom-field interaction. By considering the variance of the atomic populations, we show that "noise spectroscopy" is sensitive to the field statistics of the laser. We specifically consider the cases of resonance fluorescence (analogous in the weak-field limit to analysis by a Fabry-Pérot interferometer), two-photon excitation, and double optical resonance for variable laser intensity and bandwidth. We show that large differences in the "noise" spectra can occur between lasers characterized by a phase-diffusion or a phase-jump model, although these models would give the same values for the mean atomic populations. We believe that observation of population fluctuations can become a useful method for characterizing laser noise.

I. INTRODUCTION

During the last decade we have gained considerable understanding of the effect of laser-light fluctuations in nonlinear optical processes.[1-9] On the theoretical side methods have been developed to describe the dynamics of atoms in stochastic laser fields with amplitude and phase fluctuations.[1-6,9] Recent experiments have provided quantitative tests of these theoretical predictions.[7,8] With few exceptions,[10] however, this theoretical work has been confined to the calculation of expectation values of the physical observables, such as mean values of atomic populations. In the present paper we will be concerned with noise-induced variances (errors) of the stochastic observables around their mean values.

Our work is motivated by recent experiments with diode laser,[11] where fluctuations in the fluorescence of laser-excited atoms have been observed which can be attributed to noise in the laser field. Here again a key role is played by the nonlinearity of the atom-field interaction. To aid in the understanding and interpretation of these experimental results, we study in this paper laser-noise-induced variances of the fluorescence signal. According to the theory of a single-mode diode laser, operated not too far above threshold, the laser fluctuations can be modeled by a rotating-wave Van der Pol oscillator which predicts a slow diffusion of the laser phase and rapid (small) fluctuations of the laser amplitude around a mean value.[12,13] In the following we assume a laser with constant amplitude and fluctuating phase. We adopt two models of phase noise, a phase-diffusion model (PDM) (Refs. 1, 5, and 9) and a phase-jump model (PJM),[1,2] which assumes uncorrelated random jumps of the laser phase (see also Refs. 3 and 4). According to laser theory,[11] one expects the PDM to correspond more closely to the physical situation. We include a comparison with the PJM, however, because it predicts the same averaged populations (mean fluorescence) as the PDM in a one-photon transition, while—as we will see below—the fluctuation properties of the signal are *qualitatively* different.

The paper is organized as follows. In Sec. II we introduce the stochastic model of the laser phase noise and derive general equations for atomic averages and the variances of the atomic populations. Section III discusses fluctuations in fluorescence from a two-level system (2LS). In Sec. IV we present results for three-level systems (3LS); in particular, we study fluctuations of atomic populations in double-optical-resonance (DOR) situation,[5-7] where a lower strong noisy laser induces ac Stark splitting of an atomic transition, which can be probed by a second weak laser.

II. MODEL OF PHASE FLUCTUATIONS

The electric field of the lasers at the position of the atom has the form $\mathbf{E}(t)=\mathcal{E}(t)\epsilon e^{-i\omega t}+\text{c.c.}$ with $\mathcal{E}(t)=\mathcal{E}_0 e^{-i\Phi(t)}$ where $\mathcal{E}_0$ is a constant amplitude, ϵ is a polarization vector, and ω is the mean frequency of the light. We assume that the laser phase $\Phi(t)$ follows a Markov process. Its probability density $P(\Phi,t)$ obeys a master equation[2]

$$\frac{\partial}{\partial t}P(\Phi,t)=-bP(\Phi,t)+\frac{b}{2\pi}\int_{-\pi}^{\pi}d\Phi' f(\Phi-\Phi')P(\Phi',t)\ , \tag{2.1}$$

with $P(\Phi,t)=P(\Phi+2\pi,t)$ a periodic function of the phase. Equation (2.1) describes a stochastic evolution of the laser phase, with a jump rate b and $f(\Phi-\Phi')$ the probability for the transition $\Phi\rightarrow\Phi'$. The stationary solution of Eq. (2.1) is a uniform distribution of the phase, $P_S(\Phi)=1/2\pi$. To be consistent, we require $f(\alpha)/2\pi$ to be normalized to one on the interval $0\leq\Phi<2\pi$. In the present model, two-time electric-field correlation functions have the form[2]

$$\langle [\mathcal{E}^*(t)]^n [\mathcal{E}(t')]^n \rangle = \mathcal{E}_0^{2n} e^{-b_n |t-t'|} , \tag{2.2}$$

with

$$b_n = b \left[1 - (1/2\pi) \int_{-\pi}^{\pi} d\alpha \, e^{in\alpha} f(\alpha) \right] . \tag{2.3}$$

With the assumption that $f(\alpha)$ is symmetric (i.e., jumps $\Phi \to \Phi \pm \Delta\Phi$ occur with equal probability), b_n is real and we have $b_n = b_{-n}$. The parameter b_1 may be identified with the bandwidth of the Lorentzian light spectrum. Note that $b_0 = 0$. When $f(\alpha)$ is strongly peaked in the forward direction ($\alpha \approx 0$), the master equation (2.1) reduces to a Fokker-Planck equation for a phase-diffusion model (PDM),[1,4]

$$\frac{\partial}{\partial t} P(\Phi,t) = b_1 \frac{\partial^2}{\partial \Phi^2} P(\Phi,t) , \tag{2.4}$$

and $\Phi(t)$ becomes a Wiener process obeying the Langevin equation $d\Phi(t) = (2b_1)^{1/2} dW(t)$ with $dW(t)$ a white-noise increment. In this limit the damping terms in Eq. (2.2) are

$$b_n = n^2 b_1 \ \text{(PDM)} . \tag{2.5}$$

The other limit is one of uncorrelated jumps (phase jump model, PJM), where $f(\alpha) = 1$, and Eq. (2.3) reduces to[2]

$$b_n = b_1 [1 - \delta_{n0}] \ \text{(PJM)} . \tag{2.6}$$

In the following sections we shall study the dynamics of an atom driven by the phase-fluctuating field described above; in particular we shall be concerned with calculating the averages and variances of atomic populations to which the observables are related. This will require us to solve multiplicative stochastic differential equations[13,14] of the form

$$\frac{d}{dt} u_\mu(t) = \sum_{\nu=0}^{N} [A_{\mu\nu} + \dot{\Phi}(t) B_{\mu\nu}] u_\nu(t) , \tag{2.7}$$

where $u_\mu(t)$ ($\mu = 0, 1, \ldots, N$) is a vector of atomic density-matrix elements. $\underline{A}$ and $\underline{B}$ are matrices: in the case of interest below, $\underline{B}$ has the special form $\underline{B} = i \, \mathrm{diag}(n_1, n_2, \ldots,)$ with n_μ integers. Following arguments given in Ref. 2 (see also Appendix A), averaging of Eq. (2.7) over the phase fluctuations leads to

$$\frac{d}{dt} \langle u_\mu(t) \rangle = \sum_{\nu=0}^{N} (A_{\mu\nu} - b_{n_\mu} \delta_{\mu\nu}) \langle u_\nu(t) \rangle , \tag{2.8}$$

with b_n defined in Eq. (2.3). In a similar way we can derive an equation for the variances $\langle u_\mu(t), u_{\bar{\mu}}(t) \rangle = \langle u_\mu(t) u_{\bar{\mu}}(t) \rangle - \langle u_\mu(t) \rangle \langle u_{\bar{\mu}}(t) \rangle$,

$$\begin{aligned} \frac{d}{dt} \langle u_\mu(t), u_{\bar{\mu}}(t) \rangle = \sum_{\nu=0}^{N} \sum_{\bar{\nu}=0}^{N} & (A_{\mu\nu} \delta_{\bar{\mu}\bar{\nu}} + \delta_{\mu\nu} A_{\bar{\mu}\bar{\nu}} \\ & - b_{n_\mu} + n_{\bar{\mu}} \delta_{\mu\nu} \delta_{\bar{\mu}\bar{\nu}}) \\ & \times \langle u_\nu(t), u_{\bar{\nu}}(t) \rangle \\ & + (b_{n_\mu} + b_{n_{\bar{\mu}}} - b_{n_\mu + n_{\bar{\mu}}}) \\ & \times \langle u_\mu(t) \rangle \langle u_{\bar{\mu}}(t) \rangle , \end{aligned} \tag{2.9}$$

where the inhomogeneous terms are known from a solution of (2.8). Equation (2.9) is obtained by averaging of the stochastic equation for $u_\mu(t) u_{\bar{\mu}}(t)$ similar to Eq. (2.8) and subtracting the equation for $\langle u_\mu(t) \rangle \langle u_{\bar{\mu}}(t) \rangle$. Details of these derivations are briefly summarized in Appendix A; Eqs. (2.8) and (2.9) agree with the results of Fox[15] when our equations are specialized to a Wiener process for $\Phi(t)$.

III. POPULATION FLUCTUATIONS IN A TWO-LEVEL SYSTEM

The rate of fluorescence of a two-level system $\{ |0\rangle, |1\rangle \}$ driven by a classical field with stochastic amplitude is

$$I(t) = \kappa \rho_{11}(t) , \tag{3.1}$$

with $\rho_{11}(t)$ the population of the upper state and κ the spontaneous decay rate. (In Appendix C we show that in the weak-field limit analogous expressions result for light analyzed by a Fabry-Pérot interferometer.) Here $\rho_{11}(t)$ is obtained from the optical Bloch equations,

$$\left[\frac{d}{dt} + \begin{bmatrix} -i\Delta + \frac{1}{2}\kappa & 0 & \frac{1}{2} i \Omega e^{-i\Phi} \\ 0 & i\Delta + \frac{1}{2}\kappa & -\frac{1}{2} i \Omega e^{i\Phi} \\ i\Omega e^{i\Phi} & -i\Omega e^{-i\Phi} & \kappa \end{bmatrix} \right] \begin{bmatrix} \rho_{10} \\ \rho_{01} \\ W \end{bmatrix} = \begin{bmatrix} 0 \\ 0 \\ -\kappa \end{bmatrix} , \tag{3.2}$$

with $w(t) = \rho_{11}(t) - \rho_{00}(t)$ the population difference, $\Delta = \omega - \omega_{10}$ the detuning for resonance, and Ω the Rabi frequency. Due to fluctuations of the phase, $\rho_{11}(t)$ and $I(t)$ are stochastic functions of time. Below we are interested in the variance of the intensity fluctuations,

$$[\Delta I(t)]^2 \equiv \langle I(t), I(t) \rangle = \kappa^2 \langle \rho_{11}(t), \rho_{11}(t) \rangle , \tag{3.3}$$

around the mean value $\langle I(t) \rangle = \kappa \langle \rho_{11}(t) \rangle$. (See Appendix A.) We emphasize that Eq. (3.3) explicitly excludes quantum (shot) noise associated with emission (detection) of individual resonance fluorescence photons; instead we view $I(t)$ in Eq. (3.1) as a stochastic variable which is a functional of the laser phase. This picture is appropriate when fluorescence from a large number of atoms is considered.

The transformations $\tilde{\rho}_{10}(t)=\rho_{10}(t)e^{i\Phi(t)}$ and $\tilde{\rho}_{01}(t)=\rho_{01}(t)e^{-\Phi(t)}$ in the Bloch equations (3.2) result in a stochastic differential equation of the form (2.7). Averaging over the phase fluctuations thus given

$$\left[\frac{d}{dt}+\begin{bmatrix} z^* & 0 & i\frac{1}{2}\Omega \\ 0 & z & -i\frac{1}{2}\Omega \\ i\Omega & -i\Omega & \kappa \end{bmatrix}\right]\begin{bmatrix} \langle\tilde{\rho}_{10}\rangle \\ \langle\tilde{\rho}_{01}\rangle \\ \langle w\rangle \end{bmatrix}=\begin{bmatrix} 0 \\ 0 \\ -\kappa \end{bmatrix}, \tag{3.4}$$

with $z=i\Delta+\frac{1}{2}\kappa+b_1$. The corresponding equations for the variances are

$$\left[\frac{d}{dt}+\begin{bmatrix} z_2^* & 0 & 0 & i\Omega & 0 & 0 \\ 0 & z_2 & 0 & 0 & -i\Omega & 0 \\ 0 & 0 & \kappa & -\frac{1}{2}i\Omega & \frac{1}{2}i\Omega & 0 \\ i\Omega & 0 & -i\Omega & z_1^* & 0 & i\frac{1}{2}\Omega \\ 0 & -i\Omega & i\Omega & 0 & z_1 & -i\frac{1}{2}\Omega \\ 0 & 0 & 0 & 2i\Omega & -2i\Omega & 2\kappa \end{bmatrix}\right]\begin{bmatrix} \langle\tilde{\rho}_{10},\tilde{\rho}_{10}\rangle \\ \langle\tilde{\rho}_{01},\tilde{\rho}_{01}\rangle \\ \langle\tilde{\rho}_{10},\tilde{\rho}_{01}\rangle \\ \langle\tilde{\rho}_{10},w\rangle \\ \langle\tilde{\rho}_{01},w\rangle \\ \langle w,w\rangle \end{bmatrix}=\begin{bmatrix} (2b_1-b_2)\langle\tilde{\rho}_{10}\rangle\langle\tilde{\rho}_{10}\rangle \\ (2b_1-b_2)\langle\tilde{\rho}_{01}\rangle\langle\tilde{\rho}_{01}\rangle \\ 2b_1\langle\tilde{\rho}_{10}\rangle\langle\tilde{\rho}_{01}\rangle \\ 0 \\ 0 \\ 0 \end{bmatrix}, \tag{3.5}$$

with $z_1=i\Delta+3\kappa/2+b_1$ and $z_2=2i\Delta+\kappa+b_2$. The first three equations in (3.5) couple to the average atomic polarization and determine the time evolution of the polarization noise, which in term drives the atomic population fluctuations. Note that the source terms are proportional to the bandwidth of the light.

In the long-time limit the differential equations (3.4) and (3.5) reduce to systems of linear equations with the solutions

$$\langle\rho_{11}\rangle=\tfrac{1}{2}\frac{\Omega^2(\kappa/2+b_1)}{\kappa[\Delta^2+(\kappa/2+b_1)^2]+\Omega^2(\kappa/2+b_1)}, \tag{3.6}$$

and

$$\Delta\rho_{11}^2\equiv\frac{1}{4}\langle w,w\rangle=\frac{\Omega^4}{8\kappa}\langle w\rangle^2\frac{\mathrm{Re}\left[\left[z_1+\frac{\Omega^2}{z_2}\right]\left[\frac{2b_1-b_2}{z_1^*z_2^*}+\frac{2b_1}{\kappa|z_1|^2}\right]\right]}{\left|z_1+\frac{\Omega^2}{z_2}+\frac{\Omega^2}{\kappa}\right|^2-\left[\frac{\Omega^2}{\kappa}\right]^2}. \tag{3.7}$$

In contrast to the upper-state population (3.6) which depends only on the bandwidth b_1, the variance $\Delta\rho_{11}$ is both a function of b_1 and b_2, i.e., for a given bandwidth the PDM and the PJM predict the same population averages,[2,5] but the fluctuation properties are different. Since b_2 occurs, we see that the variance depends on the fourth-order field correlation function.

Figures 1 and 2 are plots of $\langle\rho_{11}\rangle$ (dotted line) and $\Delta\rho_{11}$ for the PDM (dashed line) and the PJM (solid line) as a function of detuning Δ for different Rabi frequencies and bandwidths. Figures 1(a)–1(c) show $\langle\rho_{11}\rangle$ and $\Delta\rho_{11}$ for a small bandwidth $b_1=0.25\kappa$ and increasing Rabi frequencies (a) $\Omega=0.25\kappa$, (b) $\Omega=1.5\kappa$, and (c) $\Omega=3\kappa$. In the plots of the population averages this increase of the intensity is reflected in a power broadening of the atomic resonance line. For weak fields [Fig. 1(a)] $\Delta\rho_{11}$ shows a distinctly different behavior in the PDM and PJM. For the phase diffusing light $\Delta\rho_{11}$ is a two-peaked curve with maxima at values of the detuning where the slope of $\langle\rho_{11}\rangle$ has its largest value, while for a jumping laser phase the maximum fluctuations occur at line center. With increasing intensity the fluctuations in the PJM develop a three-peaked structure [Fig. 1(b)]. For large saturation parameters the fluctuations are suppressed at $\Delta=0$ for the PDM and PJM, and both models show a qualitatively similar behavior for the noise [Fig. 1(c)]. For bandwidths larger than the spontaneous decay rate ($b_1=3\kappa$) and weak fields ($\Omega=1.5\kappa$), on the other hand, both models predict maximum fluctuations at the center of the atomic line (Fig. 2), and the complicated pattern of Figs. 1(a) and 1(b) disappear. For large bandwidths and strong saturation of the atom, we again find a double-peaked noise spectrum similar to the one shown in Fig. 1(c).

To understand the qualitative features in Figs. 1 and 2 we consider various limiting cases of Eq. (3.7). First we note that for weak fields $\Delta\rho_{11}$ scales proportional to Ω^2, so that the relative error $\Delta\rho_{11}/\langle\rho_{11}\rangle$ becomes independent of the light intensity. On resonance, $\Delta=0$, Eq. (3.7) reduces to

$$\Delta\rho_{11}^2=\frac{\Omega^4\kappa}{8}\frac{1}{[\Omega^2+(\kappa/2+b_1)\kappa]^2}\times\frac{(4b_1-b_2)\kappa+2b_1b_2}{[\Omega^2(3\kappa+2b_2)+\kappa(3\kappa/2+b_1)(\kappa+b_2)]}. \tag{3.8}$$

From Eq. (3.8) we see that for large Rabi frequencies the fluctuations tend to zero as $\Delta\rho_{11} \propto 1/\Omega$. Physically, this corresponds to the fact that for strong saturation the upper and lower atomic state population become approximately equal, $\rho_{11}(t) \approx \rho_{00}(t) \approx \frac{1}{2}$, an equilibrium which is only weakly perturbed by external field fluctuations. For large bandwidths ($b_1 \gg \kappa$), Eq. (3.8) is independent of b_2 and $\Delta\rho_{11}$ becomes the same in both models (compare Fig. 2). For the PDM the first term in the denominator of Eq. (3.8) becomes zero, $4b_1 - b_2 = 0$. Thus for small bandwidths $b_1 \ll \kappa$ and $\Delta = 0$ we have $(\Delta\rho_{11})_{\mathrm{PDM}}/(\Delta\rho_{11})_{\mathrm{PJM}} = 8b_1/3\kappa \ll 1$. This explains the dip in $\Delta\rho_{11}$ in Fig. 1(a) for the PDM at line center [which should not be confused with the saturation dip in Fig. 1(c). Far off resonance the relative error in the population fluctuations is

$$\Delta\rho_{11}/\langle\rho_{11}\rangle = [(b_1(2\kappa + b_1) - \tfrac{1}{4}\kappa b_2)/(\tfrac{1}{2}\kappa + b_1)^2]^{1/2}, \tag{3.9}$$

which for large bandwidths ($b_1 \gg \kappa$) is independent of b_2 (compare Fig. 2), while for small bandwidths the ratio of the relative error of the PJM and PDM approaches $(\frac{7}{4})^{1/2}$ [Fig. 1(c)].

The above discussion assumes a detector with a response time much faster than all time scales of field fluctuations and the atomic dynamics. In Appendix B we show how to generalize these results to include a finite integration time of the detection device. Physically, a finite response time of the detector tends to reduce the fluctuations; as shown by numerical calculations (see Appendix B), the qualitative features of the population fluctuations on detuning, Rabi frequency, and bandwidth as given in Figs. 1 and 2 remain essentially unchanged.

Equations (3.4) and (3.5) are easily generalized to two-photon absorption[8] from the ground state to the upper state of 2LS which is depleted by spontaneous decay to a third level (from which the electron returns to the ground state). Essentially this amounts to the replacements $b_n \to b_{2n}$ in Eqs. (3.4) and (3.5), and reinterpretation of Ω and Δ as the two-photon Rabi frequency and detuning, respectively. For the PDM this substitution is equivalent to increasing the bandwidth by a factor of 4 when compared with one-photon absorption, while the fluctuations in the PJM are the same in both cases. Thus, in two-photon absorption population fluctuations tend to be larger for the PDM than for the PJM with the same bandwidth.

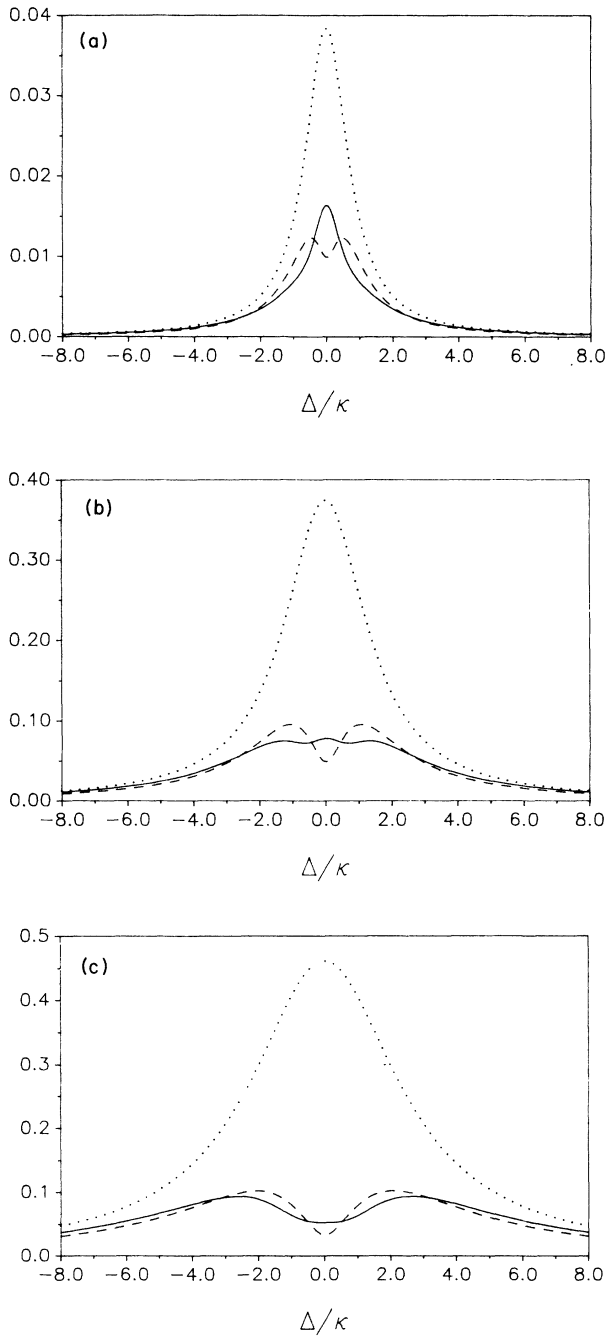

FIG. 1. Mean population $\langle\rho_{11}\rangle$ of the upper level of the 2LS (dotted line) and corresponding fluctuations $\Delta\rho_{11}$ for the PDM (dashed line) and PJM (solid line) as a function of the detuning Δ in units of κ [Eqs. (3.6) and (3.7)]. The parameters are (a) $b_1 = 0.25\kappa$ and $\Omega = 0.25\kappa$, (b) $\Omega = 1.5\kappa$, (c) $\Omega = 3\kappa$.

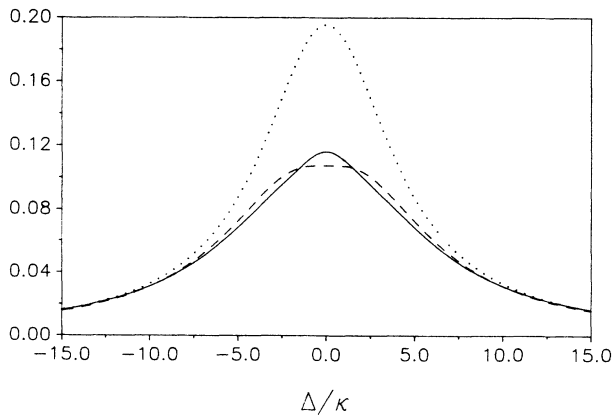

FIG. 2. Same as in Fig. 1, with $b_1 = 3\kappa$ and $\Omega = 1.5\kappa$.

IV. POPULATION FLUCTUATIONS IN DOUBLE OPTICAL RESONANCE

Bandwidth and laser line-shape effects in averaged atomic populations of three-level systems have been discussed extensively in the literature.[5-7] Below we give a brief summary of the basic equations and physical ideas of double optical resonance DOR to the extent that they provide the background of our present discussion of laser noise-induced population fluctuations.

We consider an atom with a ground state $|0\rangle$ and excited states $|1\rangle$ and $|2\rangle$. The excited states $|1\rangle$ and $|2\rangle$ have natural decay widths κ_1 and κ_2. We assume that the first transition $|0\rangle \rightarrow |1\rangle$ is strongly driven by the phase-fluctuating laser field described in Sec. II. ac Stark splitting can be observed by monitoring the population induced in level $|2\rangle$ (which is coupled via a dipole transition to $|1\rangle$) by a second laser as a function of detuning of the probe frequency. In order not to perturb the ac Stark splitting of the two-level system $\{|0\rangle, |1\rangle\}$, we adopt a weak probe approximation, i.e., we neglect the depopulation of the first excited state. For the slowly varying density-matrix elements we then find the following equations:

$$\left[\frac{d}{dt}+\kappa_2\right]\rho_{22}=\tfrac{1}{2}i\Omega'\rho_{12}+\text{c.c.}\ ,$$

$$\left[\frac{d}{dt}+i\Delta_2+\tfrac{1}{2}\kappa_{12}\right]\rho_{12}=-\tfrac{1}{2}i\Omega'\rho_{11}+\tfrac{1}{2}i\Omega e^{-i\Phi(t)}\rho_{02}\ , \tag{4.1}$$

$$\left[\frac{d}{dt}+i\Delta_1+i\Delta_2+\tfrac{1}{2}\kappa_{02}\right]\rho_{02}=-\tfrac{1}{2}i\Omega'\rho_{01}+\tfrac{1}{2}i\Omega e^{i\Phi(t)}\rho_{12}\ ,$$

with $\kappa_{ij}=\kappa_i+\kappa_j$. $\Delta_1=\omega-\omega_{10}$ and $\Delta_2=\omega'-\omega_{21}$ are the detunings of the first and second transition, respectively; Ω' is the Rabi frequency of the probe laser. The density matrix elements $\rho_{11}(t)$ and $\rho_{10}(t)$ are given as solutions of the two-level density-matrix equation (3.4). The probe laser is assumed to be monochromatic.

The transformation $\tilde{\rho}_{20}=\rho_{20}e^{i\Phi}$ reduces the density-matrix equation (4.1) to a multiplicative stochastic differential equation of the form (2.7). The atomic population averages are obtained from Eq. (2.8) with the result[5]

$$\langle\rho_{22}\rangle=\tfrac{1}{4}\frac{(\Omega')^2}{\kappa_2}\left[\tfrac{1}{2}\frac{\Omega^2}{2\kappa_1|R|^2/(R+R^*)+\Omega^2}\right]\times\frac{T+R^*\kappa_2/(R+R^*)}{ST+\frac{1}{4}\Omega^2}+\text{c.c.}\ , \tag{4.2}$$

where $R=\frac{1}{2}\kappa_{01}+b_1+i\Delta_1$, $S=\frac{1}{2}\kappa_{12}+i\Delta_2$, and $T=\frac{1}{2}\kappa_{02}+b_1+i\Delta_1+i\Delta_2$. Note that $\langle\rho_{22}\rangle$ is independent of b_2, so that the PDM and PJM again predict identical averages. For a Rabi frequency Ω much larger than the atomic decay constants κ_{ij} and bandwidth b_1, the population $\langle\rho_{22}\rangle$ as a function of Δ_1 shows two peaks which are separated approximately by $(\Omega^2+\Delta_1^2)^{1/2}$. For nonresonant excitation the doublet spectrum is asymmetric. If the detuning Δ_1 is larger than both the atomic natural linewidths κ_{ij}, the laser bandwidth b_1, and the Rabi frequency Ω, one of the absorption peaks occurs at a probe frequency offset $\Delta_2\approx-\Delta_1$ corresponding to coherent two-photon absorption; the other peak at $\Delta_1\approx0$ is associated with a two-step process whereby the probe laser excites atoms from the intermediate $|1\rangle$ state. While for small bandwidth the two-photon peak dominates the spectrum (what is referred to as the normal peak asymmetry), in a spectrally broad laser the intermediate state can become populated directly through the absorption of a photon from the wing of the laser spectrum. Thus the two-step process can dominate two-photon absorption and the peak height asymmetry is reversed, an interpretation which was substantiated by recent experiments.[7]

Equations for the population fluctuations in ρ_{22} corresponding to the density-matrix equations (4.1) and (3.2) can be obtained from Eq. (2.9). In view of the large number of the density-matrix elements and the associated loss of immediate physical insight we refrain from reproducing these equations in detail. Below we discuss results obtained by numerical solution of these equations.[16]

Figures 3–5 show plots of the mean population $\langle\rho_{22}\rangle$ (dotted line) and the variances $\Delta\rho_{22}$ for a PDM (dashed lines) and PJM (solid lines) as a function of detuning Δ_2 of the probe laser for various Rabi frequencies Ω and bandwidths b_1. In these figures we have chosen equal decay rates $\kappa_1=\kappa_2=\kappa$.[16]

Figures 3 and 4 show the spectrum when the first strong laser is tuned on resonance ($\Delta_1=0$). In fig. 3 the lower (pump) laser is assumed to be weak ($\Omega_1=0.3\kappa$) and to have a small bandwidth ($b_1=0.3\kappa$), so that $\langle\rho_{22}\rangle$ shows a single resonance line with width dominated by spontaneous decay. For both models the population fluctuations are maximum at resonance which is in contrast

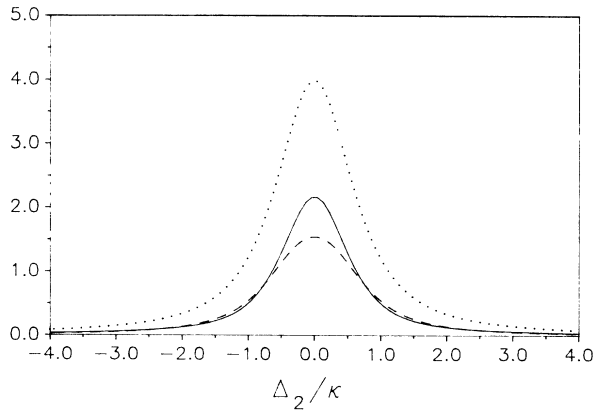

FIG. 3. Mean population $\langle\rho_{22}\rangle$ of the uppermost level in DOR (dotted line) and corresponding fluctuations $\Delta\rho_{22}$ for the PDM (dashed line) and PJM (solid line) as a function of the detuning Δ_2 of the probe laser, in units of $\Omega'^2/\kappa_1\kappa_2(\kappa_1=\kappa_2=\kappa)$. The parameters are $\Delta_1=0$, $\Omega_1=0.3\kappa$, and 0.3κ. $\langle\rho_{22}\rangle$ and $\Delta\rho_{22}$ are multiplied by a scale factor 10^2.

to the situation in the 2LS [compare Fig. 1(a)]; however, further calculations reveal that a double-peaked fluctuation spectrum reminiscent of the results of the 2LS is obtained for the PDM at considerably smaller pump bandwidth b_1.

Increasing the intensity of the first laser, the spectrum exhibits ac Stark splitting. In Fig. 4(a) we have chosen $b_1=0.3\kappa$ and $\Omega_1=3\kappa$. For the PJM the fluctuations are three peaked with maxima at the positions of ac-Stark-split states $\Delta_2\approx\pm\frac{1}{2}\Omega$ and at $\Delta_2=0$. By contrast, in the PDM the variances show four peaks: for each of the doublet lines of $\langle\rho_{22}\rangle$ we find two maxima at detunings where the slope of $\langle\rho_{22}\rangle$ is largest with a deep minimum at $\Delta_2=0$; the two middle peaks (closer to $\Delta_2=0$) become more pronounced as the bandwidth b_1 decreases. Additional calculations have shown that for large Rabi frequencies the central peak ($\Delta_2=0$) for the PJM disappears. Increasing the bandwidth b_1 [Fig. 4(b) with $b_1=3\kappa$ and $\Omega_1=3\kappa$] washes out the ac Stark splitting while the fluctuations show a doublet structure with virtually no differences between the predictions of both the PJM and the PDM; in a field with a still larger bandwidth this double hump disappears and we find a single-peaked fluctuation spectrum.

In Fig. 5 we plot the off-resonance spectrum for a detuning $\Delta_1=7\kappa$, a Rabi frequency $\Omega_1=3\kappa$, and bandwidth

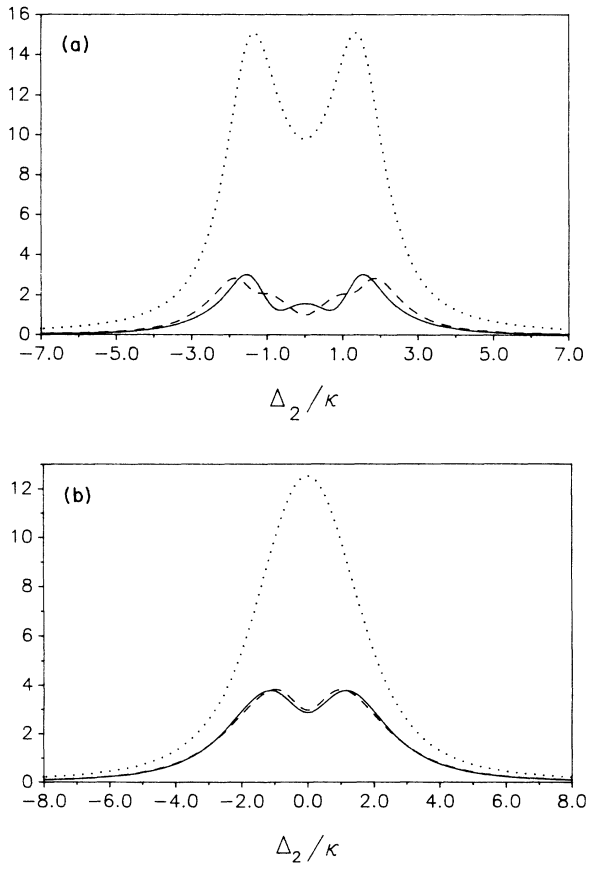

FIG. 4. Same as in Fig. 3. The parameters are (a) $\Delta_1=0$, $\Omega_1=3\kappa$, $b_1=0.3\kappa$, and (b) $b_1=3\kappa$. The scale factor is 10^2.

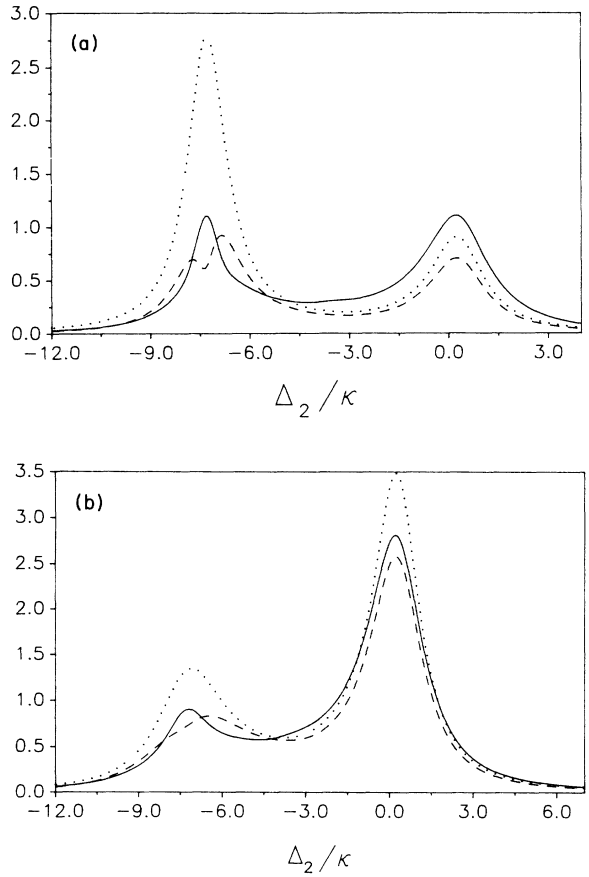

FIG. 5. Same as in Fig. 3. The parameters are (a) $\Delta_1=7\kappa$, $\Omega_1=3\kappa$, $b_1=0.2\kappa$, and (b) $b_1=\kappa$. The scale factor is 10^2.

$b_1=0.2\kappa$ [Fig. 5(a)] and $b_1=\kappa$ [Fig. 5(b)]. The two peaks in $\langle\rho_{11}\rangle$ correspond to two-photon absorption ($\Delta_1=-\Delta_2$) and the two-step process ($\Delta_1=0$). For the small bandwidth [Fig. 5(a)] the peak at $\Delta_2=-\Delta_1$ dominates; the fluctuations in the PJM show a maximum at line center while the PDM again exhibits a asymmetric doublet structure. Fluctuations at $\Delta_2=0$ are surprisingly large, in particular for the PJM (a property which becomes even more pronounced at smaller bandwidth). For bandwidths $b_1>\frac{1}{2}\kappa$ the peak asymmetry reverses and the two-step process dominates the two-photon peak [Fig. 5(b) with $b_1=\kappa$]. In this case the fluctuation properties of both PDM and PJM are similar with maxima at the line centers of the doublet.

V. CONCLUSIONS

We have shown that fluctuations in the observed intensity, when light from a noisy laser is scattered by an atomic system, are sensitive to the field statistics of the laser. These fluctuations were obtained by considering the variances of the atomic populations, which depend on higher-order field correlation functions than the mean populations. Of particular interest is the difference between the observed "noise" for the phase-diffusion and phase-jump models, illustrated in Figs. 1 and 2 for the

2LS. For small bandwidths and low intensities [Fig. 1(a)], the PDM shows maxima in the wings at the points where the slope of the scattered intensity, $\kappa\langle\rho_{11}\rangle$, as a function of detuning is maximum. This is to be expected, since the intensity at these point is most sensitive to small changes in frequency (and hence phase). In contrast, the PJM, which has the same average population $\langle\rho_{11}\rangle$, shows a maximum at line center. The reason for this is that the PJM changes in phase, when they occur, are large (being random modulo 2π), so that jumps to all points in the profile occur, in contrast to the continuous small phase excursions of the PDM which are sensitive to the region of maximum slope. For broad-band radiation, as shown in Fig. 2, large changes in frequency (phase) also occur for the PDM and then the maximum "noise" also occurs at line center.

The results presented for fluorescence (in the weak-field limit equivalent to transmission through a Fabry-Perot interferometer), two-photon excitation, and DOR as a function of bandwidth and laser intensity for the PDM and PJM (Figs. 1–5) indicate a wealth of interesting features, which are not revealed by just examining the average populations. In fact, the two-photon excitation, since it is characterized by higher-order field correlation functions, is even more sensitive than the one-photon fluorescence for the PDM. We therefore believe that "noise spectroscopy" provides an excellent method for characterizing laser-field statistics. The feasibility of such noise spectroscopy has, of course, been shown by the experiments of Wieman and Tanner and Holberg,[11] although for precise measurements it will be necessary for the frequency response of the detection system to exceed the bandwidth and relaxation rates.

ACKNOWLEDGMENTS

We thank C. Wieman, C. Tanner, L. Holberg, and L. Westling for discussions which stimulated this work. Th.H. was supported by the Austrian Ministry for Science and Research. H.R. acknowledges support from the Austrian Science Foundation. J.C. was supported by National Science Foundation Grant No. PHY-86-04504. P.Z. acknowledges financial support by the JILA Visiting Fellow program.

APPENDIX A

With the definitions $\bar{u}_\mu(t)=e^{-in_\mu\Phi(t)}u_\mu(t)$ and $A_{\mu\nu}(\Phi)=e^{-in_\mu\Phi}A_{\mu\nu}e^{in_\nu\Phi}$, Eq. (2.7) is equivalent to the stochastic equation

$$\frac{d}{dt}\bar{u}_\mu(t)=\sum_{\nu=0}^{N}A_{\mu\nu}(\Phi(t))\bar{u}_\nu(t)\ ,$$

which, together with the phase $\Phi(t)$, defines a Markov process $\{\bar{u}_\mu(t),\Phi(t)\}$ with probability density $P(\bar{u}_\mu,\Phi,t)$. This probability density is a solution of the master equation

$$\frac{\partial}{\partial t}P(\bar{u}_\mu,\Phi,t)=\left[-\sum_{\mu=0}^{N}\sum_{\nu=0}^{N}\frac{\partial}{\partial\bar{u}_\mu}A_{\mu\nu}(\Phi)\bar{u}_\nu+L(\Phi)\right]\times P(\bar{u}_\mu,\Phi,t)\ , \tag{A1}$$

with $L(\Phi)$ the master operator of the phase [defined by the right-hand side of Eq. (2.1)].

Multiplying Eq. (A1) by $e^{-in_\mu\Phi}\bar{u}_\mu$ and integrating over the $\bar{u}$'s and the phase Φ, we derive Eq. (2.8) for the averages $\langle u_\mu(t)\rangle$. In a similar way, Eq. (2.9) for the variances by obtained by multiplying Eq. (A1) by $e^{-i(n_\mu+n_\nu)\Phi}\bar{u}_\mu\bar{u}_\nu$ and again integrating over the whole phase space.

In the long-time limit the atomic mean values and variances settle down to a stationary state. In view of the normalization $\sum_j\rho_{jj}(t)=1$ of the density-matrix elements, we can define the first component of the u vector as $u_0(t)=\sum_j\rho_{jj}(t)$, so that $u_0(t)=1$ for all times, and we have $\langle u_0,u_\mu\rangle=0(\mu=0,1,\ldots,N)$. This results in a system of linear equations for the $N(N+1)/2$ variances $\langle u_m,u_n\rangle(m,n=1,2,\ldots,N)$. Note that $(\langle u_m,u_n\rangle)$ is a (symmetric semipositive) covariance matrix. For the 2LS we have to solve a 6×6 [see Eq. (3.5)], for the 3LS a 36×36 system of linear equations.

APPENDIX B: DETECTOR WITH FINITE INTEGRATION TIME

The theory developed in Sec. III assumes that the response time of the detector is much faster than the time scale of fluctuations. A phenomenological model for a detector with a finite integration time is readily constructed by writing for the measured intensity

$$I_D(t)=\Gamma\int_{-\infty}^{t}dt'\,e^{-\Gamma(t-t')}I(t')\ , \tag{B1}$$

with $1/\Gamma$ the response time and $I(t)$ given by Eq. (3.1). From Eq. (B1) we have in the stationary limit $\langle I_D(t)\rangle=\langle I(t)\rangle$ for the mean value of the fluorescence with $\langle I(t)\rangle=\kappa\langle\rho_{11}(t)\rangle$. According to Eq. (B1), the variance can be calculated from the atomic correlation function $\langle\rho_{11}(t),\rho_{11}(t')\rangle$. Alternatively, an equation for the variance is readily obtained by augmenting the stochastic Bloch equations (3.2) by

$$\frac{d}{dt}I_D(t)=-\Gamma I_D(t)+\Gamma I(t) \tag{B2}$$

and deriving an equation for $\langle I_D(t),I_D(t)\rangle$ according to (2.9). In the long-time limit we find

$$\langle I_D(t),I_D(t)\rangle=\tfrac{1}{2}\kappa\langle I_D(t),w(t)\rangle\ , \tag{B3}$$

with

$$\begin{bmatrix}\langle I_D,\tilde{\rho}_{10}\rangle\\ \langle I_D,\tilde{\rho}_{01}\rangle\\ \langle I_D,w\rangle\end{bmatrix}=\tfrac{1}{2}\kappa\Gamma\left[\Gamma+\begin{bmatrix}z^* & 0 & \frac{1}{2}i\Omega\\ 0 & z & -\frac{1}{2}i\Omega\\ i\Omega & -i\Omega & \kappa\end{bmatrix}\right]^{-1}\times\begin{bmatrix}\langle\tilde{\rho}_{10},w\rangle\\ \langle\tilde{\rho}_{01},w\rangle\\ \langle w,w\rangle\end{bmatrix}\ . \tag{B4}$$

The right-hand side of Eq. (B4) is known from (3.5) of Sec. III; in particular we note that the matrix in Eq. (B4) is identical to the matrix in Eq. (3.4) which governs the time evolution of the averaged stochastic density matrix. According to Eqs. (B3) and (B4), the fluctuations in the fluorescence are reduced when Γ becomes comparable or smaller than b, κ, or Ω. Numerical calculations based on Eqs. (B3) and (B4) show for finite Γ that the figures in Sec. III remain essentially unchanged, apart from an overall reduction factor in the fluctuation.

The above discussion can be adapted to more complicated models of the detector response, e.g., filtering by a Fabry-Pérot interferometer.

APPENDIX C: COMPARISON WITH A FABRY-PÉROT

In this appendix we compare our results for the variance of fluorescence from a 2LS (Sec. III) with the fluctuations in the output from a Fabry-Pérot interferometer, driven by the same noisy laser. The output amplitude $\mathcal{E}_{\rm out}(t)$ from a Lorentzian through pass filter obeys the equation

$$\frac{d}{dt}\mathcal{E}_{\rm out}(t)=(i\Delta-\Gamma)\mathcal{E}_{\rm out}(t)+\Gamma\mathcal{E}_{\rm in}(t)\ , \tag{C1}$$

with $\mathcal{E}_{\rm in}(t)=\mathcal{E}_0 e^{-i\Phi(t)}$ the complex incoming field amplitude, Δ the detuning of the mean frequency of the incoming laser field from the resonance frequency of the Fabry-Pérot, and Γ the damping coefficient of the cavity. The variances in the output intensity $I_{\rm out}(t)=|\mathcal{E}_{\rm out}(t)|^2$ are easily calculated in analogy to our treatment of the 2LS in Sec. III. With the definitions $z=i\Delta+\Gamma+b_1$, $z_1=i\Delta+3\Gamma+b_1$, and $z_2=2i\Delta+2\Gamma+b_2$ the intensity fluctuations of a Fabry-Pérot interferometer are determined by the formula

$$(\Delta I_{\rm out})^2=\frac{(2\Gamma\mathcal{E}_0)^4}{8(2\Gamma)}\frac{1}{|z_1|^2}\times\mathrm{Re}\left[z_1\left[\frac{2b_1-_2}{z^{2*}z_2^*}+\frac{2b_1}{2\Gamma|z|^2}\right]\right]\ . \tag{C2}$$

This agrees with the weak-field limit of Eq. (3.7) for the 2LS, i.e., when we take the limit of small Rabi frequencies $\Omega\to 0$, and when we make the identifications $\kappa\to 2\Gamma$ and $\Omega\to 2\mathcal{E}_0\Gamma$. We emphasize, however, that a Lorentzian through pass filter and a 2LS in a weak light field give identical results only when the spontaneous decay width of the atom is identical to the damping constant of the Fabry-Pérot interferometer.

---

*Permanent address: Institute for Theoretical Physics, University of Innsbruck, A-6020 Innsbruck, Austria.

[1]For a review, see P. Zoller, in *Multiphoton Processes*, edited by P. Lambropoulos and S. J. Smith (Springer-Verlag, Berlin, 1984), Vol. 2, p. 68; for a fairly complete list of references see also Ref. 2.

[2]A. I. Burshtein, A. A. Zharikov, and S. I. Temkin, J. Phys. B (to be published).

[3]L. D. Zusman and A. I. Burshtein, Zh. Eksp. Teor. Fiz. **61**, 976 (1971) [Sov. Phys.—JETP **34**, 520 (1972)]; P. Zoller and F. Ehlotzky, J. Phys. B **10**, 3023 (1977).

[4]B. W. Shore, J. Opt. Soc. Am. B **1**, 176 (1984); K. Wodkiewicz, B. W. Shore, and J. H. Eberly, *ibid.* B **1**, 398 (1984); Phys. Rev. A **30**, 2390 (1984).

[5]A. T. Georges and P. Lambropoulos, Phys. Rev. A **18**, 587 (1978).

[6]S. N. Dixit, P. Zoller, and P. Lambropoulos, Phys. Rev. A **21**, 1289 (1980).

[7]M. W. Hamilton, K. Arnett, S. J. Smith, D. S. Elliott, M. Dziemballa, and P. Zoller, Phys. Rev. A **36**, 178 (1987).

[8]D. S. Elliott, M. W. Hamilton, K. Arnett, and S. J. Smith, Phys. Rev. Lett. **53**, 439 (1984).

[9]G. S. Agarwal and C. V. Kunasz, Phys. Rev. A **27**, 996 (1983).

[10]P. Zoller, J. Phys. B **15**, 2911 (1983).

[11]C. Wieman and C. Tanner (private communciation); L. Holberg (private communication).

[12]H. Haken, *Handbuch der Physik* (Springer-Verlag, Berlin, 1973), Vol. XXV/2c.

[13]M. Osinski, IEEE J. Quant. Electron. **QE-23**, 9 (1987).

[14]N. G. van Kampen, *Stochastic Processes in Physics and Chemistry* (North-Holland, Amsterdam, 1981); P. Zoller, Phys. Rev. A **20**, 1019 (1979).

[15]R. F. Fox, J. Math. Phys. **13**, 1196 (1972).

[16]In practice it turns out to be simpler to solve the three-level system equations for the variances without the weak-probe approxiamtion. We produced Figs. 3–5 with the assumption $\Omega'=0.01\kappa$.